# Response of human iPSC-cardiomyocytes to adrenergic drugs assessed by high-throughput pericellular oxygen measurements

Weizhen Li, David McLeod, Yuli W. Heinson,
Matthew W. Kay, Zhenyu Li, and Emilia Entcheva*

Department of Biomedical Engineering
School of Engineering and Applied Science
The George Washington University
Washington, DC 20052

*Correspondence:

Emilia Entcheva, entcheva@gwu.edu

## ABSTRACT

Rate-modulating drugs, such as adrenergic agonists and antagonists, are widely used in the treatment of cardiovascular conditions. Preclinical assessment of new rate and metabolism modulators can be augmented through the development of high-throughput (HT) methods that allow chronic measurements. Such approaches are best coupled with human induced pluripotent stem cell-derived cardiomyocytes (hiPSC-CMs) – a scalable experimental model of the human heart. Here, we evaluate the utility of long-term optical (label-free) measurements of pericellular oxygen in a HT format (96-well plates) for the assessment of the effectiveness of adrenergic drugs in hiPSC-CMs. Quantitative metrics were derived from these long-term measurements, e.g. steady-state pericellular oxygen and time to reach 5%, and we sought correlation to measurements performed in the same samples using all-optical electrophysiology. Adrenergic agonists significantly increased oxygen consumption rate, and this was best seen in the kinetics of initial depletion of pericellular oxygen, i.e. time to reach 5%. Adrenergic antagonists decreased oxygen consumption rate and their action was best quantified using steady-state values for pericellular oxygen after at least 5 hours. Drug type identification based on oxygen consumption rate correlated well with the acute measurements of spontaneous rate in the same samples. Furthermore, we showed that direct rate modulation with chronic optogenetic pacing detectably sped up the oxygen consumption rate and optogenetic transformation did not interfere with classification of adrenergic drugs. We conclude that HT label-free optical oxygen measurements may be a valuable approach for long-term non-invasive monitoring of the action of rate- and metabolism-modulating drugs in preclinical studies.

**Keywords:** optical oxygen sensors, pericellular oxygen, all-optical electrophysiology, human iPSC-CMs, high-throughput plates, adrenergic agonists, beta blockers

## INTRODUCTION

Modulation of heart rhythm by the sympathetic nervous system (SNS) through action on the adrenergic receptors is an essential physiological response. Catecholamines like norepinephrine and epinephrine target adrenergic receptors to trigger systemic fight-or-flight response, which includes increase in heart rate, contractility and energy consumption. In 1948, Ahlquist(Ahlquist 1948) categorized the adrenergic receptors into two distinct types, $\alpha$- and $\beta$-adrenergic, based on their pharmacological responsiveness and sensitivity to stimulation by various catecholamines. Subsequent studies have identified them as G-protein coupled receptors (GPCRs)(Caron, Srinivasan et al. 1979, Dixon, Kobilka et al. 1986), and divided them into nine subtypes ($\alpha$1A, $\alpha$1B, $\alpha$1D, $\alpha$2A, $\alpha$2B, $\alpha$2C, $\beta$1, $\beta$2, $\beta$3)(Brodde and Michel 1999). The adrenoreceptor subtypes most prevalent in the human heart are $\beta_1$ and $\beta_2$, with lower presence of $\alpha$1 subtypes (Bristow, Ginsburg et al. 1986, Brodde 1993, Brodde and Michel 1999). The physiological activation of cardiac adrenoreceptor $\alpha_1$ and $\beta_1$ yields positive inotropic and chronotropic effects ($\beta_1 >> \alpha_1$), inducing increased muscle performance and cardiac hypertrophy. Conversely, adrenergic antagonists slow down heart rate and overall metabolism.

Clinically, the regulation of cardiac adrenoreceptors has broad applications and therefore the development of respective pharmacological agents has been of great interest. Beta-adrenergic antagonists/blockers are among the most successful cardiac drugs in use(Bristow 2011). Currently, there are over a dozen $\beta$-adrenergic blockers approved by the FDA for various cardiac conditions, including hypertension, angina pectoris, cardiac arrhythmias, hypertrophic cardiomyopathy, and heart failure, among others. Beta-blockers are also used to treat non-cardiac conditions, such as glaucoma and muscle tremors. On the other hand, $\beta$-adrenergic agonists act similarly to norepinephrine and epinephrine, increasing cardiac contractility, muscle performance and heart rate. They are clinically used to treat bradycardia, asthma, chronic obstructive pulmonary disease, and allergic reactions(Ortega and Peters 2010). There is interest in developing receptor specific rate-modulating drugs. Therefore, high-throughput methods for reliable and fast preclinical testing of candidate compounds are desirable.

Human-induced pluripotent stem cell-derived cardiomyocytes (hiPSC-CMs) offer scalability and relevance to human physiology. These characteristics make them an attractive model for high-throughput (HT) preclinical drug cardiotoxicity screening(Blinova, Schocken et al. 2019). In addition, hiPSC-CMs derived from patients with genetic cardiac diseases can recapitulate aspects of patient's specific response to pharmacological perturbations(Burridge, Li et al. 2016). This scalable experimental model of the human heart can be coupled with HT technology for drug screening applications, offering new options for the human-centered modernization proposed by the FDA and NIH(Ahmed, Shivnaraine et al. 2023). Electromechanical activity in cardiomyocytes is the major contributor to their oxygen consumption (>80% is attributed to contraction)(Keeley and Mann 2019). This study aimed to assess the applicability of longitudinal HT optical imaging of pericellular oxygen (in 96-well plates)(Li, McLeod et al. 2023, Li, McLeod et al. 2025) as a label-free method to detect the action of adrenergic drugs in human iPSC-CMs, cross-validated with measurements of action potentials and spontaneous rates using all-optical electrophysiology(Heinson, Han et al. 2023) in the same samples.

## MATERIALS AND METHODS

### Human iPSC-CM culture

Human iPSC cardiomyocytes (iCell Cardiomyocytes[2] from CDI/Fujifilm) were used in this study. Cells were thawed as per manufacturer's protocol and plated at 50,000 cells per 96-well ($1.56 \times 10^5$ cells / $cm^2$) to form a syncytium. Glass-bottom 96-well plates were with attached oxygen sensors, covering half of each well, were sterilized and fibronectin coated before cell plating, as described previously(Li, McLeod et al. 2023, Li, McLeod et al. 2025). Cells were cultured for 5 days with culture medium exchange every other day before experiments. Pre-treatment oxygen consumption was measured a day in advance, after cell medium exchange.

### Treatment with adrenergic drugs

Adrenergic agonists isoproterenol (Sigma-Aldrich I6504) and phenylephrine (Sigma-Aldrich P6126) were used at a dosage of 10 μM applied for 24 hours. Adrenergic antagonists sotalol (Sigma-Aldrich cardiotoxicity ligand set) and propranolol (Sigma-Aldrich P0884) were used at a dosage of 30 μM and 10 μM for 24 hours respectively. Isoproterenol and phenylephrine were diluted in sterile water (Sigma-Aldrich W4502). Sotalol and propranolol were prepared in DMSO (Invitrogen D12345) with a final concentration of 0.3% and 0.1%. As a negative control, we incorporated samples treated with 0.3% DMSO for comparison. All prepared drug solutions were filtered with 0.2 μm sterile filter (VWR 101093-372) before application. Culture medium volume was 200 μL for all samples.

### Optical measurements of pericellular oxygen and data analysis

Pericellular oxygen was measured using Ruthenium-based oxygen sensing film and a camera system (PreSens, Germany) in the 37ºC humidified incubator with 5% $CO_2$, as described previously(Li, McLeod et al. 2023, Li, McLeod et al. 2025). The exposure time was set to 0.8 s and oxygen images were taken every 5 min in this study. The measurement is based on fluorescence quenching by oxygen and absolute values of pericellular oxygen can be extracted from the acquired images based on the Stern-Volmer equation and a two-point calibration procedure(Peniche Silva, Liebsch et al. 2020, Li, McLeod et al. 2023). Time-dependent oxygen calibration was applied in the first two hours of recording, considering temperature and humidity changes from ambient to incubator. Whole-plate data normalization was applied to avoid negative values in the oxygen reading and to set the maximum oxygen reading to be equilibrium oxygen concentration in 37ºC, 5% $CO_2$ humidified incubator, at 18.6%(Keeley and Mann 2019).

### High throughput all-optical electrophysiology

Voltage and calcium transients were measured optically using fluorescent reporters and a high-throughput whole plate imaging(Han, Heinson et al. 2023, Heinson, Han et al. 2023). After adrenergic treatment, samples were labeled with membrane voltage dye BeRST1 at 1 μM (Ex/Em 660/680nm, from Evan W. Miller, University of California, Berkeley) and calcium dye Rhod-4 AM at 10 μM (Ex/Em 660/680nm, AAT Bioquest). Signals were acquired at 100 frames per second and transients were extracted and analyzed, as done previously(Liu, Han et al. 2023). These electromechanical

measurements were done 24 h after the initial application of the adrenergic modulators and with re-application immediately before the recordings.

### In-incubator optical pacing with pericellular oxygen monitoring

To enable optical pacing, hiPSC-CMs were infected with adenovirus Ad-CMV-hChR2-eYFP(Ambrosi and Entcheva 2014) five days after cell plating, and drug treatment was done two days later. A blue LED light source was mounted above the PreSens oxygen measuring system in the incubator. The illuminated area was adjusted to cover 12 samples at intensity 0.13-0.3 mW/ $mm^2$. Optical pacing was conducted for about 5 hours at 1Hz with 10ms pulse duration, and optical sensing of oxygen was continuous with images acquired every 2 min.

### Statistical analysis

Statistical analyses were performed with GraphPad Prism 7. Grouped bar-dot plots were presented as mean $\pm$ SD with individual data points. Ordinary one-way ANOVA with Dunnett's correction for group-wise comparison were applied to identify statistical significance between the control group and treatment groups. Linear regression was applied when correlating the pericellular oxygen results and the electrophysiological measurements.

### Immunolabeling and cell imaging

Mouse monoclonal anti-$\alpha$-actinin primary antibody (Sigma-Aldrich A7811) and goat anti-mouse Alexa fluor 647 secondary antibody (ThermoFisher A21235) were used for human iPSC-CMs alpha actinin labeling. Hoechst 33342 (ThermoFisher 62249) was used for labeling the cell nuclei. Human iPSC-CMs on glass bottom 96-well plate were imaged with Zeiss spinning disk confocal microscope. Human iPSC-CMs grown on oxygen sensors were imaged with Leica multi-photon confocal microscope with a water immersion objective.

## RESULTS

### Integrated system for HT long-term oxygen measurements with all-optical electrophysiology for acute and chronic assessment of adrenergic agonists and antagonists.

Pharmaceutical agents targeting adrenergic receptors are a clinically important drug category in active development, including vasopressors, bronchodilators, and controllers of cardiac rhythm. Considering that over 80% of the cardiomyocyte oxygen consumption is related to mechanical contraction, we tested if measurements of pericellular oxygen can be used to quantify the effectiveness of adrenergic agonists and antagonists. To validate the drug treatments, we used sequential optical measurements of pericellular oxygen followed by all-optical electrophysiology in the same samples (in 96-well glass-bottom plates), as shown in **Fig. 1.** Since the oxygen sensors are non-transparent, we used laser-cut semicircles to cover half of each well and allow unimpeded optical electrophysiology measurements in the other half (**Fig. 2A**).

The oxygen sensor is about 180 µm thick, with an oxygen-sensitive layer, a polyester support layer, and a white optical isolation layer. It has a ruthenium-based oxygen-responsive dye and a reference dye. Cells grow directly on top of the oxygen permeable white optical isolation layer, allowing for continuous pericellular oxygen readings (**Fig. 2B**). Images of hiPSC-CMs grown directly on the glass-bottom of 96-well plate and on the oxygen sensor are shown in **Fig. 2C, D** (alpha actinin in red, nuclei in blue with 20 µm scale bar). Within a well, the densely plated cardiomyocytes formed a contiguous layer (syncytium) across the sensor-covered portion and the other half.

**Adrenergic agonists accelerate oxygen consumption while adrenergic antagonists slow down oxygen consumption; different features of the oxygen depletion curve best differentiate their action from control**

Two adrenergic agonists, a β-agonist, isoproterenol (10µM) and an α1-agonist, phenylephrine (10µM), and two β-adrenergic antagonists, sotalol (30µM) and propranolol (10µM), were applied on hiPSC-CMs for up to 24 hours based on the reported studies summarized in **Table 1**. DMSO control with 0.3% DMSO in culture medium was included to consider its potential influence as a solvent. Pre-treatment oxygen consumption showed similar trend across all samples with steep oxygen depletion in the first 3 hours and stabilization after that, as we have shown previously. After 10 hours, some samples exhibited non-monotonic oxygen consumption behavior as we have reported before(Li, McLeod et al. 2023, Li, McLeod et al. 2025).

Following adrenergic treatment, the initial rate of depletion of pericellular oxygen as well as the steady state levels were greatly affected (**Fig. 3A, B**). **Fig. 3C** summarizes pericellular oxygen levels of hiPSC-CMs at 6.5 and 22 hours after different treatments. Compared to control, adrenergic agonists accelerated oxygen depletion. The 30 µM sotalol treatment slowed down the initial oxygen consumption (in the first 5 h), but steady state levels (after 22 h) were similar to control. The 10 µM propranolol treatment slowed down oxygen consumption consistently, evidenced by continuous high pericellular oxygen readings at 5 h and at 22 h. One-way ANOVA with Dunnett's multiple comparisons suggested statistical significance between control and all treatments (at $p<0.01$), see figure legend for details.

To capture the change in rate of depletion we identified two metrics - time to reach 5% and 2% $O_2$ - as sensitive to adrenergic modulators (**Fig. 3D**). Adrenergic agonists isoproterenol and phenylephrine accelerated the depletion of pericellular oxygen to below 5% to 1.5 hours in average, and 86% (26 out of 31) of isoproterenol treated and 97% (30 out of 31) of the phenylephrine treated samples reached hypoxic levels - 2% $O_2$ – in less than 3 hours after media change. In comparison, the average time to reach 5% $O_2$ among the control samples was 4.7 hours and 69% (20 out of 29) didn't reach 2% $O_2$. Among sotalol treated samples 64%(16 out of 25) reached 5% $O_2$, and the average time to do so was 6.1 h; 61% of sotalol treated samples (16 out of 26) didn't reach 2% $O_2$. For propranolol treated samples, 7% (2 out of 26) reached 5% $O_2$ and none of them reached hypoxic levels, i.e. <2% $O_2$. For DMSO control, 54% samples (12 out of 22) reached 5% $O_2$ in an average of 6.51 hours, and 83% (19 out of 23) didn't reach 2% $O_2$. Based on previous studies, sotalol (membrane impermeable) is a less potent β-blocker compared

to propranolol (membrane permeable), which may explain its milder effects of pericellular oxygen(Shannon, Bare et al. 2022).

In summary, adrenergic antagonists (β-blockers) were most easily distinguishable by the higher steady-state values for pericellular oxygen within 5 h post-treatment, while the adrenergic agonists had a distinct signature in the time to reach 5% of pericellular oxygen (significantly faster than other groups).

**Adrenergic perturbations modify electromechanical responses of human iPSC-CMs, including beat rate, action potential and calcium transient morphologies.**

High-throughput all-optical electrophysiology platform was deployed for electrophysiology functional assessment. Spontaneous activity was documented by measuring membrane voltage and intracellular calcium separately (**Fig. 4A**). Comparison of spontaneous frequency, after normalization by the average rate of control samples, is shown in **Fig. 4B**. On average, 10 μM isoproterenol and 10 μM phenylephrine increased spontaneous rate by 59% and 52% respectively (n=12 to 16 per group). The 30 μM sotalol treatment decreased spontaneous rate by 45% on average (n=12). And the 10 μM propranolol treatment completely suppressed spontaneous activity in 85% (n=16) of the samples. DMSO (at 0.3%) reduced spontaneous activity by 25% on average (n=8). The multiple comparison of one-way ANOVA analysis showed statistically significant difference for isoproterenol, phenylephrine, and propranolol with respect to control (at $p<0.02$), see figure legend for details.

We also compared action potential duration (APD80) and calcium transient duration (CTD80), **Fig. 4C**. These rate-uncorrected APD80 and CTD80 showed prolongation in samples treated with adrenergic antagonists compared to the control, with statistically significant difference for sotalol and for propranolol with respect to control (at $p<0.001$). The adrenergic agonists, as used here, did not significantly affect APD and CTD.

**Correlation between oxygen consumption and electromechanical function in hiPSC-CMs indicates the overall impact of adrenergic perturbations.**

We sought to uncover potential correlation in oxygen consumption and electromechanical activity in the cardiomyocytes. Pericellular oxygen levels at 5 h after adrenergic treatments were plotted against spontaneous beating frequency within the same samples to probe for such correlation in the iPSC-CMs (**Fig. 5A**). A decrease in 5h pericellular oxygen level correlated with an increase in spontaneous rate. This trend was expected as cardiac electromechanical activity is the dominant process underlying oxygen consumption. Adrenergic antagonist propranolol treated samples had the lowest spontaneous activity level and the highest 5 h pericellular oxygen levels, followed by sotalol treated samples. Non treated and DMSO control samples were in the middle of the trend, and adrenergic agonists isoproterenol and phenylephrine presented increased spontaneous activity levels and low 5 h pericellular oxygen levels. Grouping the samples by treatment type, revealed more clearly the trends induced by the adrenergic perturbations (**Fig. 5B**). When this metric was used (pericellular oxygen levels 5 h after treatment), the adrenergic antagonists were clearly identifiable, while the adrenergic

agonists, despite the induction of higher rates in the treated samples, were less distinct from controls. The morphology of the response curves can be further used to extract the most sensitive features to correctly identify adrenergic drugs, i.e. time to reach 5% would have been a better metric for adrenergic agonists, as seen in **Fig. 3**.

**Active optical pacing directly impacts oxygen consumption. Responses of hiPSC-CMs to adrenergic perturbations are preserved after optogenetic transduction.**

To confirm the effect of heart rate on oxygen consumption in hiPSC-CMs in a more direct way, we paced the cells directly using optogenetic stimulation. Cells were made light-sensitive through ChR2-eYFP transduction prior to experiments, which we have shown to not cause any electrophysiological side effects(Klimas, Ambrosi et al. 2016). Considering potential interference (by the optogenetic actuator or its reporter) on the optical oxygen measurements, we first confirmed that the modified iPSC-CMs have preserved sensitivity to the adrenergic modulators (**Fig. 6A-B**). Just as seen with unmodified myocytes, adrenergic agonists accelerated initial oxygen depletion (in the first 2 hours), while the application of adrenergic antagonists led to high steady-state levels of pericellular oxygen (around 10%) (n=5 per group).

To test the effects of pacing on oxygen consumption, we deployed the setup, Illustrated in **Fig. 6C**, where a blue LED was used above the 96-well plate for optical pacing, while optical probing of oxygen consumption was done by the system positioned underneath the 96-well plate. Part of the 96-well plate was covered with black tape to block the blue light stimulation and have control (spontaneously beating) samples and actively paced (at 1Hz) samples. In **Fig. 6D**, we show the pericellular oxygen readouts from the optically paced and non-paced samples within 5 h of active optical pacing. Pacing accelerated oxygen consumption and resulted in lower pericellular oxygen readout compared to spontaneously beating control samples in the same plate. The readouts at 2 h are quantified in **Fig. 6E**, where the paced cells have depleted oxygen more than controls, albeit statistical significance was not reached. However, the two groups had statistically different time to reach 5% $O_2$ (n=4 per group, $p = 0.0338$), just as we saw that this metric is better in distinguishing the action of adrenergic agonists (**Fig. 3**). This confirmed similarity between adrenergic agonists and active pacing as accelerators of oxygen consumption rate.

## DISCUSSION

In this study we explored the question if label-free chronic optical observation of oxygen consumption in cardiomyocytes can be used to successfully differentiate the action of rate-modulating drugs (adrenergic agonists and antagonists). Such approach has multiple advantages, including: 1) simplicity (can be implemented in a very low cost, compact format), 2) scalability (all measurements reported here are in standard 96-well plates with a whole-plate readout), 3) no interference with cellular function (no dyes or modifications are needed), 4) compatibility with long-term monitoring (suitable for days to months of cellular observation as various treatments are applied), and 5) sophistication

of captured parameters (multiple metrics can be extracted that quantify metabolic function from the relatively simple measurements).

In previous work, we have validated that the method can be used to report true absolute values of oxygen, just as a classic electrochemical Clark electrode can, with the benefit that it can be calibrated to track changes in oxygen in the tight pericellular space (immediately surrounding the cells), where Clark electrodes are not applicable(Li, McLeod et al. 2023). We have shown the method to be able to capture quantitative differences in oxygen consumption in human cardiac fibroblasts and human iPSC-cardiomyocytes and distinguish states of normoxia, hyperoxia and hypoxia(Li, McLeod et al. 2025). Furthermore, a substantial increase in metabolism could be captured in iPSC-CMs over five days in culture, with clear differences depending on the conditions of growth, with the cells grown in conditions close to normoxia showing the greatest improvement(Li, McLeod et al. 2025). Our results of cardiac cell oxygenation in HT plates brought about important insights and some surprising observations, e.g. we found hyperoxic state for cardiac fibroblast growth and for sparse cardiomyocyte cultures, yet highly hypoxic conditions were observed for static cardiomyocyte cultures when grown in dense syncytia. These previous investigations gave us confidence that this HT approach has great potential in tracking metabolic cardiac cell responses over time and can be leveraged in drug development.

With the knowledge that cardiomyocytes are highly metabolically active cells with their electromechanical activities using over 80% of the oxygen, we focused on rate-modulating drugs and their signature in the measured oxygen consumption curves. A cross-validation of the activity of the adrenergic agonists and antagonists on the iPSC-CMs was done in the same samples (from which optical oxygen measurements were obtained) using HT all-optical cardiac electrophysiology. Future investigations can provide more time-resolved direct validation using concurrent measurements of oxygen and electrophysiology over time. However, even for the single timepoint measures of rate, our approach here yielded convincing correlation between rate of electromechanical activity and metrics extracted from the oxygen consumption curves. Using optogenetic pacing over several hours, we confirmed heart rate was indeed a key driver of the level of depletion of pericellular oxygen in the iPSC-CMs. In terms of useful metrics for future drug testing studies, we found that adrenergic antagonists, such as β-blockers, are best distinguished by the steady-state levels of pericellular oxygen within several hours of treatment (and depending on dose, perhaps earlier). Adrenergic agonists were best identified by the time to reach 5% (or hypoxic levels of 2%) of pericellular oxygen, which directly relates to the initial rate of depletion. The same was true for differentiating the actively paced cells from spontaneously active cells. Future work can expand the panel of metabolic compounds tested and use the entire shape (temporal profiles) of pericellular oxygen curves in conjunction with machine learning algorithms(Lubba, Sethi et al. 2019) for building classifiers and more sensitive predictors of drug action in cardiomyocytes, as well as for quality control of various metabolic maturation strategies(Feyen, McKeithan et al. 2020, Nikitina, Roysam et al. 2023) for human iPSC-CMs. With high interest in

development of rate-control drugs and metabolic modulators, we envision the reported method to be widely applicable, with high translational potential, especially with the focus on human-based preclinical investigations(Ahmed, Shivnaraine et al. 2023).

**Data Availability:** The data underlying this study are available in the published article.

**Conflict of Interest**: The authors declare no conflict of interest.

**Acknowledgements:** This work was supported in part by grants from the NIH-NHLBI R01HL144157 and from the NSF EFMA1830941. Biorender was used to create parts of figures 1, 2, 3 and 6.

## REFERENCES


1. Ahlquist, R. P. (1948). "A STUDY OF THE ADRENOTROPIC RECEPTORS." American Journal of Physiology-Legacy Content **153**(3): 586-600.
2. Ahmed, S. M., R. V. Shivnaraine and J. C. Wu (2023). "FDA Modernization Act 2.0 Paves the Way to Computational Biology and Clinical Trials in a Dish." Circulation **148**(4): 309-311.
3. Ambrosi, C. M. and E. Entcheva (2014). "Optogenetic control of cardiomyocytes via viral delivery." Methods Mol Biol **1181**: 215-228.
4. Blazeski, A., R. Zhu, D. W. Hunter, S. H. Weinberg, E. T. Zambidis and L. Tung (2012). "Cardiomyocytes derived from human induced pluripotent stem cells as models for normal and diseased cardiac electrophysiology and contractility." Prog Biophys Mol Biol **110**(2-3): 166-177.
5. Blinova, K., D. Schocken, D. Patel, C. Daluwatte, J. Vicente, J. C. Wu and D. G. Strauss (2019). "Clinical Trial in a Dish: Personalized Stem Cell-Derived Cardiomyocyte Assay Compared With Clinical Trial Results for Two QT-Prolonging Drugs." Clin Transl Sci **12**(6): 687-697.
6. Bristow, M. R. (2011). "Treatment of Chronic Heart Failure With β-Adrenergic Receptor Antagonists." Circulation Research **109**(10): 1176-1194.
7. Bristow, M. R., R. Ginsburg, V. Umans, M. Fowler, W. Minobe, R. Rasmussen, P. Zera, R. Menlove, P. Shah, S. Jamieson and et al. (1986). "Beta 1- and beta 2-adrenergic-receptor subpopulations in nonfailing and failing human ventricular myocardium: coupling of both receptor subtypes to muscle contraction and selective beta 1-receptor down-regulation in heart failure." Circ Res **59**(3): 297-309.
8. Brodde, O. E. (1993). "Beta-adrenoceptors in cardiac disease." Pharmacol Ther **60**(3): 405-430.
9. Brodde, O. E. and M. C. Michel (1999). "Adrenergic and muscarinic receptors in the human heart." Pharmacol Rev **51**(4): 651-690.
10. Burridge, P. W., Y. F. Li, E. Matsa, H. Wu, S. G. Ong, A. Sharma, A. Holmström, A. C. Chang, M. J. Coronado, A. D. Ebert, J. W. Knowles, M. L. Telli, R. M. Witteles, H. M. Blau, D. Bernstein, R. B. Altman and J. C. Wu (2016). "Human induced pluripotent stem cell-derived cardiomyocytes recapitulate the predilection of breast cancer patients to doxorubicin-induced cardiotoxicity." Nat Med **22**(5): 547-556.
11. Caron, M. G., Y. Srinivasan, J. Pitha, K. Kociolek and R. J. Lefkowitz (1979). "Affinity chromatography of the beta-adrenergic receptor." J Biol Chem **254**(8): 2923-2927.
12. Comollo, T. W., X. Zou, C. Zhang, D. Kesters, T. Hof, K. J. Sampson and R. S. Kass (2022). "Exploring mutation specific beta blocker pharmacology of the pathogenic late sodium channel current from patient-specific pluripotent stem cell myocytes derived from long QT syndrome mutation carriers." Channels **16**(1): 173-184.
13. da Rocha, A. M., J. Creech, E. Thonn, S. Mironov and T. J. Herron (2019). "Detection of Drug-Induced Torsades de Pointes Arrhythmia Mechanisms Using hiPSC-CM Syncytial Monolayers in a High-Throughput Screening Voltage Sensitive Dye Assay." Toxicological Sciences **173**(2): 402-415.
14. Dixon, R. A., B. K. Kobilka, D. J. Strader, J. L. Benovic, H. G. Dohlman, T. Frielle, M. A. Bolanowski, C. D. Bennett, E. Rands, R. E. Diehl, R. A. Mumford, E. E. Slater, I. S. Sigal, M. G. Caron, R. J. Lefkowitz and C. D. Strader (1986). "Cloning of the gene and cDNA for mammalian beta-adrenergic receptor and homology with rhodopsin." Nature **321**(6065): 75-79.
15. Feyen, D. A. M., W. L. McKeithan, A. A. N. Bruyneel, S. Spiering, L. Hörmann, B. Ulmer, H. Zhang, F. Briganti, M. Schweizer, B. Hegyi, Z. Liao, R.-P. Pölönen, K. S. Ginsburg, C. K. Lam, R. Serrano, C. Wahlquist, A. Kreymerman, M. Vu, P. L. Amatya, C. S. Behrens, S. Ranjbarvaziri, R. G. C. Maas, M. Greenhaw, D. Bernstein, J. C. Wu, D. M. Bers, T. Eschenhagen, C. M. Metallo and M. Mercola

(2020). "Metabolic Maturation Media Improve Physiological Function of Human iPSC-Derived Cardiomyocytes." Cell Reports **32**(3).
16. Földes, G., M. Mioulane, J. S. Wright, A. Q. Liu, P. Novak, B. Merkely, J. Gorelik, M. D. Schneider, N. N. Ali and S. E. Harding (2011). "Modulation of human embryonic stem cell-derived cardiomyocyte growth: a testbed for studying human cardiac hypertrophy?" J Mol Cell Cardiol **50**(2): 367-376.
17. Han, J. L., Y. W. Heinson, C. J. Chua, W. Liu and E. Entcheva (2023). "CRISPRi gene modulation and all-optical electrophysiology in post-differentiated human iPSC-cardiomyocytes." Communications Biology **6**(1): 1236.
18. Heinson, Y. W., J. L. Han and E. Entcheva (2023). "OptoDyCE-plate as an affordable high throughput imager for all optical cardiac electrophysiology." Journal of Molecular and Cellular Cardiology Plus **6**: 100054.
19. Huang, M., X. Fan, Z. Yang, L. Cyganek, X. Li, G. Yuecel, H. Lan, Y. Li, A. Wendel, S. Lang, K. Bieback, I. El-Battrawy, X. Zhou, I. Akin and M. Borggrefe (2021). "Alpha 1-adrenoceptor signalling contributes to toxic effects of catecholamine on electrical properties in cardiomyocytes." EP Europace **23**(7): 1137-1148.
20. Keeley, T. P. and G. E. Mann (2019). "Defining Physiological Normoxia for Improved Translation of Cell Physiology to Animal Models and Humans." Physiol Rev **99**(1): 161-234.
21. Kitsuka, T., M. Itoh, S. Amamoto, K.-i. Arai, J. Oyama, K. Node, S. Toda, S. Morita, T. Nishida and K. Nakayama (2019). "2-Cl-C.OXT-A stimulates contraction through the suppression of phosphodiesterase activity in human induced pluripotent stem cell-derived cardiac organoids." PLOS ONE **14**(7): e0213114.
22. Klimas, A., C. M. Ambrosi, J. Yu, J. C. Williams, H. Bien and E. Entcheva (2016). "OptoDyCE as an automated system for high-throughput all-optical dynamic cardiac electrophysiology." Nat Commun **7**: 11542.
23. Knight, W. E., Y. Cao, Y. H. Lin, C. Chi, B. Bai, G. C. Sparagna, Y. Zhao, Y. Du, P. Londono, J. A. Reisz, B. C. Brown, M. R. G. Taylor, A. V. Ambardekar, J. C. Cleveland, Jr., T. A. McKinsey, M. Y. Jeong, L. A. Walker, K. C. Woulfe, A. D'Alessandro, K. C. Chatfield, H. Xu, M. R. Bristow, P. M. Buttrick and K. Song (2021). "Maturation of Pluripotent Stem Cell-Derived Cardiomyocytes Enables Modeling of Human Hypertrophic Cardiomyopathy." Stem Cell Reports **16**(3): 519-533.
24. Li, W., D. McLeod, S. Antonevich, M. R. Pozo, Z. Li and E. Entcheva (2025). "Pericellular oxygen dynamics in human cardiac fibroblasts and iPSC-cardiomyocytes in high-throughput plates: insights from experiments and modeling." Journal of Molecular and Cellular Cardiology Plus: 100464.
25. Li, W., D. McLeod, J. T. Ketzenberger, G. Kowalik, R. Russo, Z. Li, M. W. Kay and E. Entcheva (2023). "High-throughput optical sensing of peri-cellular oxygen in cardiac cells: system characterization, calibration, and testing." Frontiers in Bioengineering and Biotechnology **11**.
26. Liu, W., J. L. Han, J. Tomek, G. Bub and E. Entcheva (2023). "Simultaneous Widefield Voltage and Dye-Free Optical Mapping Quantifies Electromechanical Waves in Human Induced Pluripotent Stem Cell-Derived Cardiomyocytes." ACS Photonics **10**(4): 1070-1083.
27. Lubba, C. H., S. S. Sethi, P. Knaute, S. R. Schultz, B. D. Fulcher and N. S. Jones (2019). "catch22: CAnonical Time-series CHaracteristics." Data Mining and Knowledge Discovery **33**(6): 1821-1852.
28. Moreau, A., J.-B. Reisqs, H. Delanoe-Ayari, M. Pierre, A. Janin, A. Deliniere, F. Bessière, A. C. Meli, A. Charrabi, E. Lafont, C. Valla, D. Bauer, E. Morel, V. Gache, G. Millat, X. Nissan, A. Faucherre, C. Jopling, S. Richard, A. Mejat and P. Chevalier (2021). "Deciphering DSC2 arrhythmogenic cardiomyopathy electrical instability: From ion channels to ECG and tailored drug therapy." Clinical and Translational Medicine **11**(3): e319.

29. Navarrete, E. G., P. Liang, F. Lan, V. Sanchez-Freire, C. Simmons, T. Gong, A. Sharma, P. W. Burridge, B. Patlolla, A. S. Lee, H. Wu, R. E. Beygui, S. M. Wu, R. C. Robbins, D. M. Bers and J. C. Wu (2013). "Screening drug-induced arrhythmia [corrected] using human induced pluripotent stem cell-derived cardiomyocytes and low-impedance microelectrode arrays." Circulation **128**(11 Suppl 1): S3-13.
30. Nikitina, A. A., T. Roysam and M. L. Kemp (2023). "Early dynamic changes in iPSC oxygen consumption rate predict future cardiomyocyte differentiation." Biotechnol Bioeng **120**(8): 2357-2362.
31. Novak, A., L. Barad, A. Lorber, M. Gherghiceanu, I. Reiter, B. Eisen, L. Eldor, J. Itskovitz-Eldor, M. Eldar, M. Arad and O. Binah (2015). "Functional abnormalities in iPSC-derived cardiomyocytes generated from CPVT1 and CPVT2 patients carrying ryanodine or calsequestrin mutations." J Cell Mol Med **19**(8): 2006-2018.
32. Ortega, V. E. and S. P. Peters (2010). "Beta-2 adrenergic agonists: focus on safety and benefits versus risks." Current Opinion in Pharmacology **10**(3): 246-253.
33. Peniche Silva, C. J., G. Liebsch, R. J. Meier, M. S. Gutbrod, E. R. Balmayor and M. van Griensven (2020). "A New Non-invasive Technique for Measuring 3D-Oxygen Gradients in Wells During Mammalian Cell Culture." Front Bioeng Biotechnol **8**: 595.
34. Shannon, T. R., D. J. Bare, S. Van Dijk, S. Raofi, T. N. Huynh, Y. K. Xiang, J. Bossuyt, K. L. Dodge-Kafka, K. S. Ginsburg and D. M. Bers (2022). "Subcellular Propagation of Cardiomyocyte β-Adrenergic Activation of Calcium Uptake Involves Internal β-Receptors and AKAP7." Function (Oxf) **3**(3): zqac020.
35. Sheng, X., M. Reppel, F. Nguemo, F. I. Mohammad, A. Kuzmenkin, J. Hescheler and K. Pfannkuche (2012). "Human pluripotent stem cell-derived cardiomyocytes: response to TTX and lidocain reveals strong cell to cell variability." PLoS One **7**(9): e45963.
36. Stillitano, F., J. Hansen, C.-W. Kong, I. Karakikes, C. Funck-Brentano, L. Geng, S. Scott, S. Reynier, M. Wu, Y. Valogne, C. Desseaux, J.-E. Salem, D. Jeziorowska, N. Zahr, R. Li, R. Iyengar, R. J. Hajjar and J.-S. Hulot (2017). "Modeling susceptibility to drug-induced long QT with a panel of subject-specific induced pluripotent stem cells." eLife **6**: e19406.
37. Toepfer, C. N., A. Sharma, M. Cicconet, A. C. Garfinkel, M. Mücke, M. Neyazi, J. A. L. Willcox, R. Agarwal, M. Schmid, J. Rao, J. Ewoldt, O. Pourquié, A. Chopra, C. S. Chen, J. G. Seidman and C. E. Seidman (2019). "SarcTrack." Circulation Research **124**(8): 1172-1183.
38. Zhao, Q., X. Wang, S. Wang, Z. Song, J. Wang and J. Ma (2017). "Cardiotoxicity evaluation using human embryonic stem cells and induced pluripotent stem cell-derived cardiomyocytes." Stem Cell Research & Therapy **8**(1): 54.

## Table 1. Adrenergic agonists and antagonists used in human iPSC-CMs

| | drugs | target receptors | dose used | reported dosages | notes | ref |
|---|---|---|---|---|---|---|
| agonists | (−)-isoproterenol hydrochloride | β | 1-10 μM | 1μM | increased calcium transient amplitude; increased max rate of rise and decay | (Novak, Barad et al. 2015) |
| | | | | 0.1-10μM | increased beat rate in 30min, recovered at 24h | (Zhao, Wang et al. 2017) |
| | | | | 1μM | positive chronotropic effect (increased beat rate) | (Sheng, Reppel et al. 2012) |
| | | | | 50μM | increased conduction velocity & increased contraction rate in 15min | (Blazeski, Zhu et al. 2012) |
| | (R)-(−)-phenylephrine hydrochloride | α1 | 10 μM | 1μM 48h | iPSC-CM maturation (increase in cell area, organized sarcomeres, hypertrophy marker ANF) | (Földes, Mioulane et al. 2011) |
| | | | | 1μM 48h | hypertrophic cardiomyopathy conditioning | (Knight, Cao et al. 2021) |
| | | | | 100μM 1h | induced Takotsubo syndrome (TTS)-like heart dysfunctions (APD-prolongation and Vmax-suppression) | (Huang, Fan et al. 2021) |
| antagonists | sotalol | β | 30 μM | 30-500μM | decreased beat rate at 30 μM; FPDc prolongation at 100 to 500 μM | (Navarrete, Liang et al. 2013) |
| | | | | 0.1-100μM | decreased beat rate; APD prolongation | (da Rocha, Creech et al. 2019) |
| | | | | 10-300μM | inter-individual differences in response to sotalol | (Stillitano, Hansen et al. 2017) |
| | (±)-propranolol hydrochloride | β | 10 μM | 10μM | inhibition of $I_{NaL}$ | (Comollo, Zou et al. 2022) |
| | | | | 1-10μM | decreased beat rate, decreased sarcomere shortening; minimal effect on duration of contraction and relaxation, except at high doses. | (Toepfer, Sharma et al. 2019) |
| | | | | 3μM | decreased beat rate | (Moreau, Reisqs et al. 2021) |
| | | | | NA | decrease in beat rate of hiPSC-CM spheroids; no effect on the total cAMP production | (Kitsuka, Itoh et al. 2019) |

## FIGURES

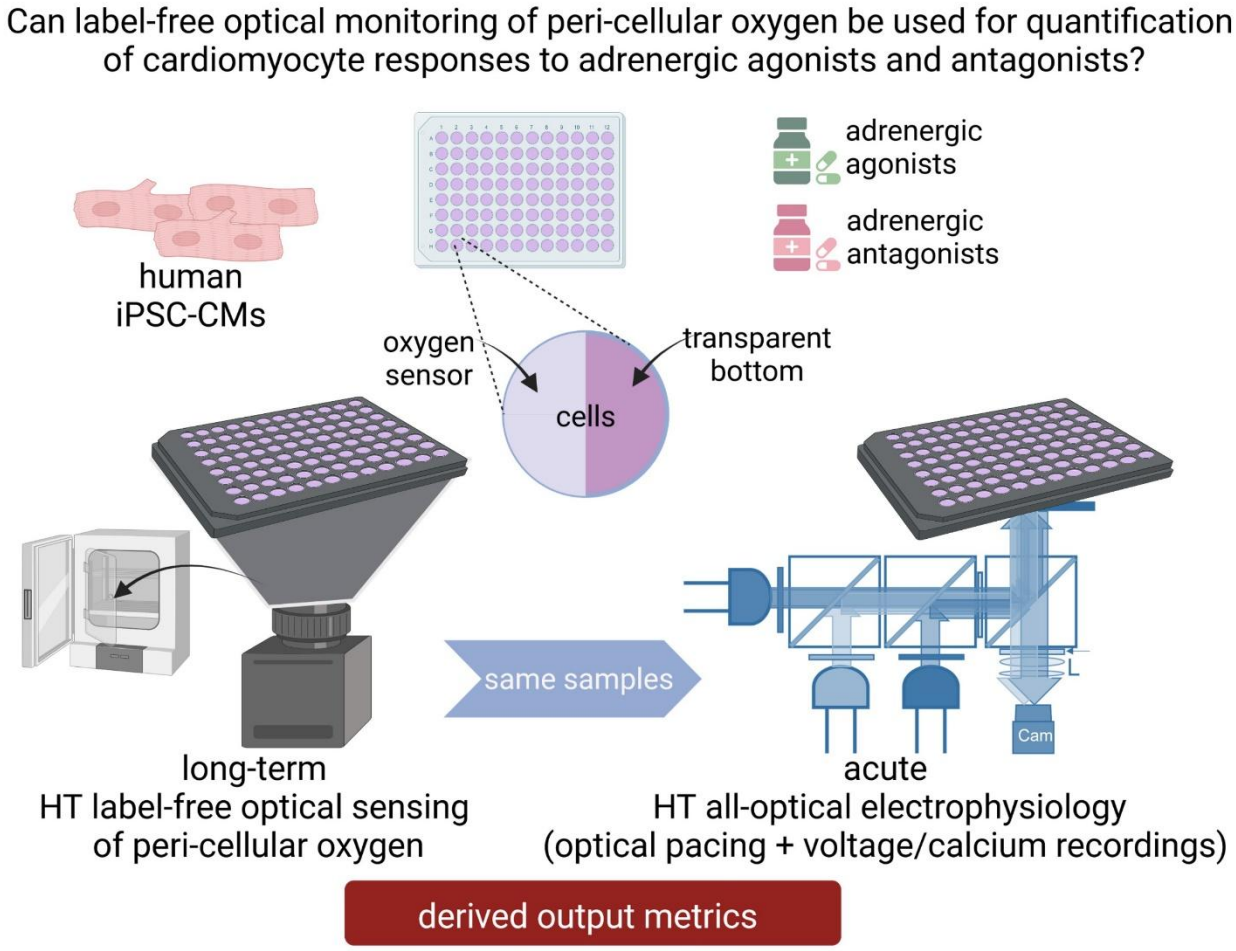


**Figure 1. Study overview.** Human induced pluripotent stem cell-derived cardiomyocytes (hiPSC-CMs) cultured in 96-well plates can be used for high-throughput (HT) drug testing. This study examines if HT label-free HT optical sensing of peri-cellular oxygen can accurately capture responses of human iPSC-CMs to adrenergic agonists and antagonists and what metrics may be most useful. The study uses acute all-optical electrophysiology in the same samples to register level of activity and correlate to peri-cellular oxygen responses.

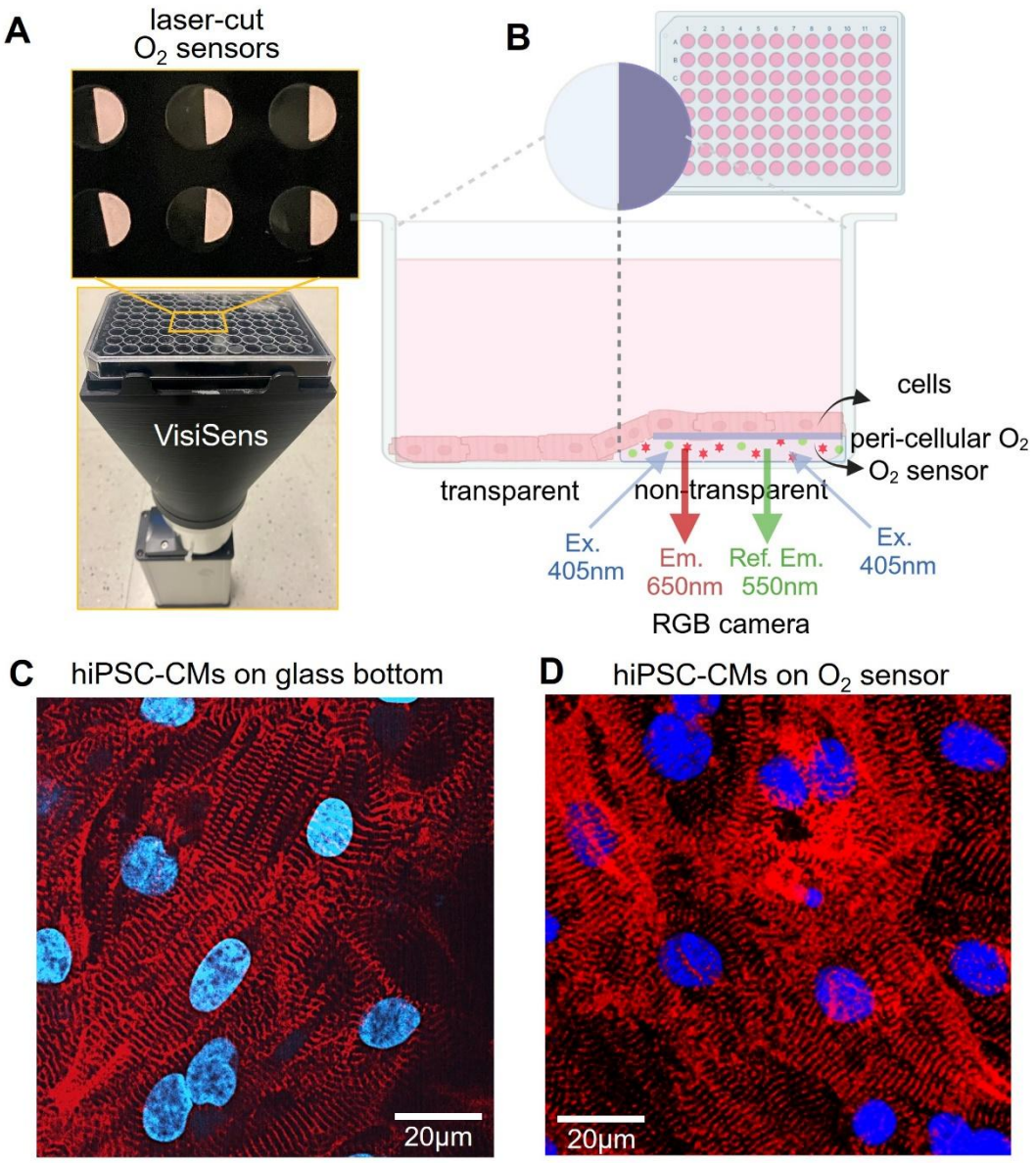


**Figure 2**. **High-throughput optical sensing of pericellular oxygen in standard 96-well plates.**

**A.** Top: bottom-up view of semi-circular oxygen sensor attached 96 well. Bottom: VisiSens 96-well plate oxygen measuring setup. **B.** Schematic of 96 well peri-cellular oxygen sensing. Cells are grown on the glass bottom on the left side for all-optical electrophysiology measuring, while on the right side, they are grown on the oxygen sensor for real-time oxygen measurements. Oxygen sensitive membrane in the oxygen sensor (pink) contains ruthenium-based oxygen-responsive dye that has fluorescent quenching with peri-cellular oxygen molecules. Under VisiSens 405nm light excitation, the 650nm red fluorescent emission indicates the oxygen level, while a 550nm reference fluorescent emission remains constant regardless of the oxygen level. **C, D.** Human iPSC-CMs cultured on the glass-bottom (C) and oxygen sensor(D). Alpha-actinin signal in red, and nuclei in blue, with 20μm scale bar.

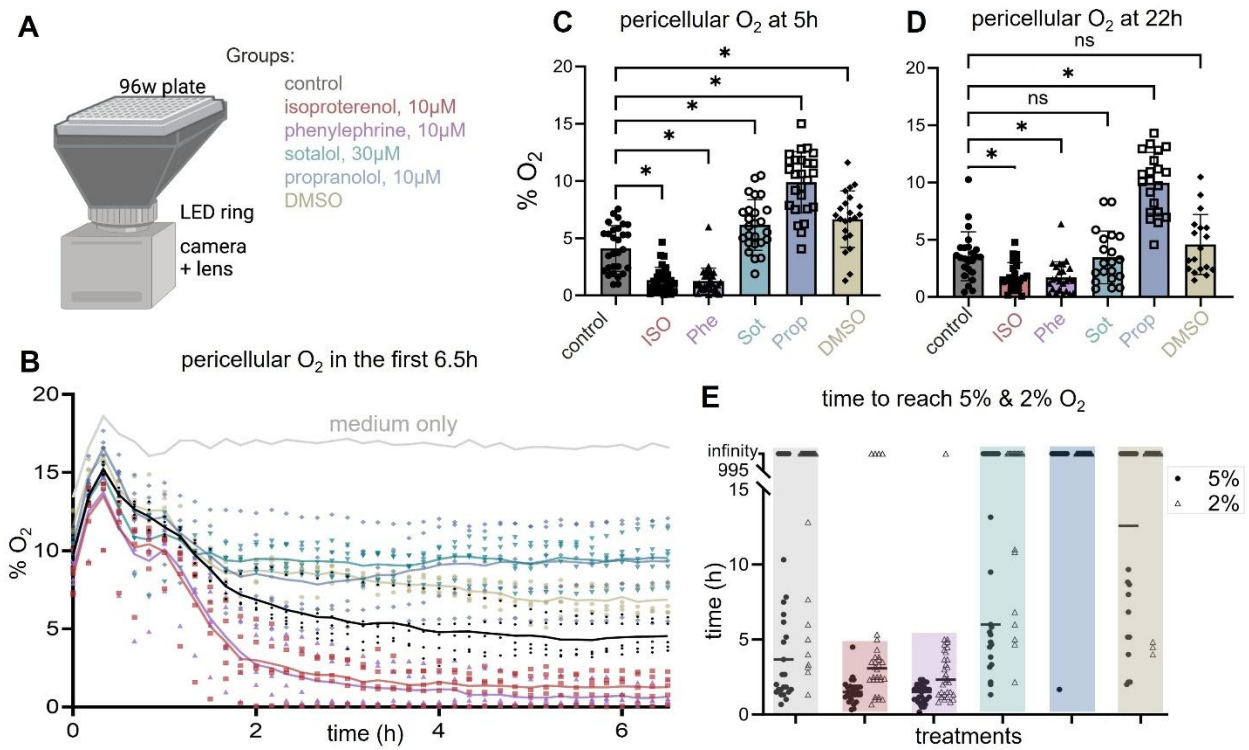


**Figure 3. Pericellular oxygen dynamics in response to adrenergic agonists and antagonists. A.** VisiSens 96-well plate oxygen measurement setup and color code for adrenergic agonists and antagonists. **B.** Pericellular oxygen readout in the first 6.5 hours of treatment with adrenergic agonists and antagonists; data presented as individual samples (wells) along with a trend line representing the average (n=5 per group, with an additional control well with culture medium only, no cells). Drug treatment was done six days after cell plating. **C.** Pericellular oxygen levels at 5 hours post-treatment (n=22-29 per group). One-way ANOVA with Dunnett's multiple comparisons showed a significant difference between control and sotalol-treated groups ($p = 0.001$), and between control and all other treatment groups ($p < 0.0001$). **D.** Pericellular oxygen levels at 22 hours post-treatment (n=18-24 per group). One-way ANOVA with Dunnett's test revealed significant differences between control and isoproterenol ($p = 0.0173$), phenylephrine ($p = 0.0096$), and propranolol ($p < 0.0001$) treated groups. **E.** Time to reach 5% and 2% pericellular oxygen (n=22-31 per group); some samples never reached below 5%.

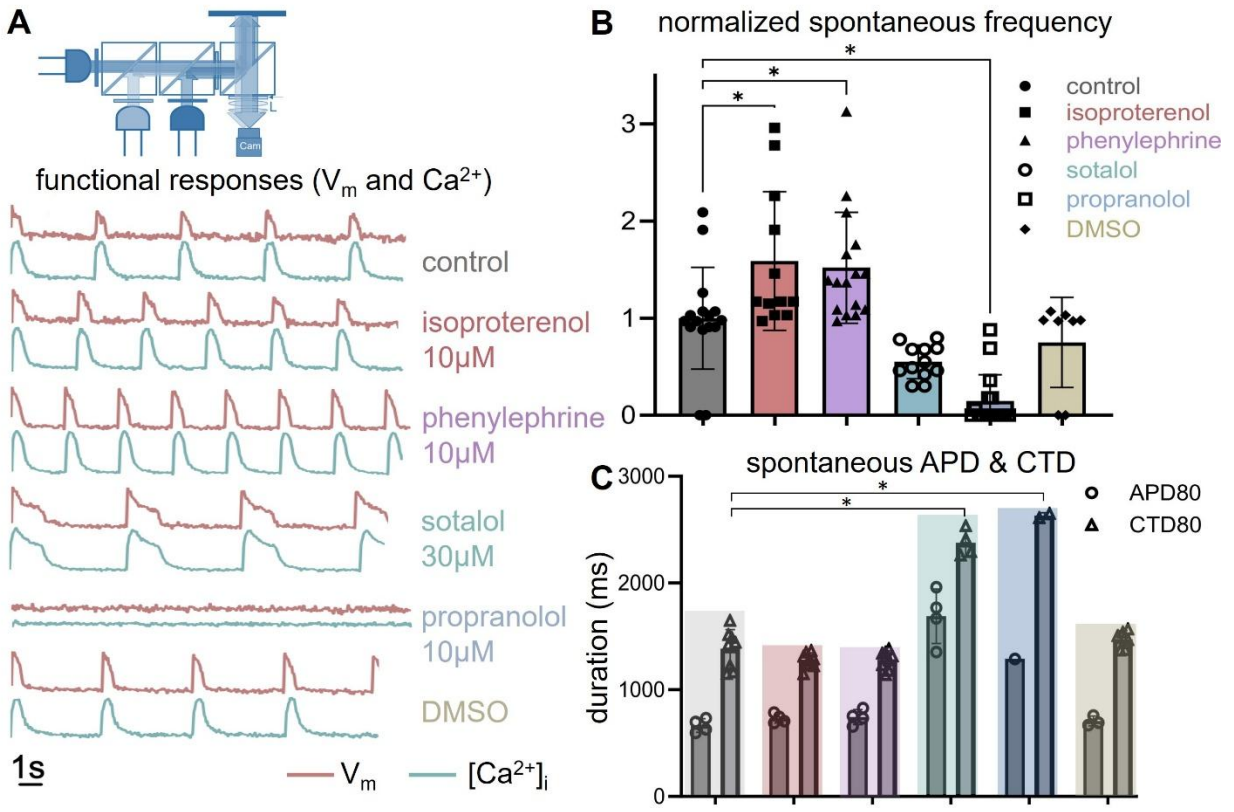


**Figure 4. Functional follow-up: voltage and calcium activities in hiPSC-CMs post-adrenergic modulation A.** Example traces from the whole-plate all-optical electrophysiology measurement, 24 h after treatment with adrenergic agonists and antagonists. Membrane voltage signal represented in red, while calcium transients are shown in green; these were measured sequentially. **B.** Normalized spontaneous beating frequency of human iPSC-CMs under adrenergic agonist and antagonist treatments (n = 8–16 per group). One-way ANOVA with Dunnett's multiple comparisons showed significant differences between control and isoproterenol ($p = 0.01$), phenylephrine ($p = 0.0159$), and propranolol ($p < 0.0001$). **C.** Human iPSC-CMs spontaneous action potential duration (APD80) and calcium transient duration (CTD80) under adrenergic agonists and antagonists' treatments (n=1-8 per group; some samples were completely quiescent). Statistical analysis of CTD80 using ordinary one-way ANOVA and multiple comparisons revealed adjusted $p<0.0001$ for control vs. sotalol and control vs. propranolol.

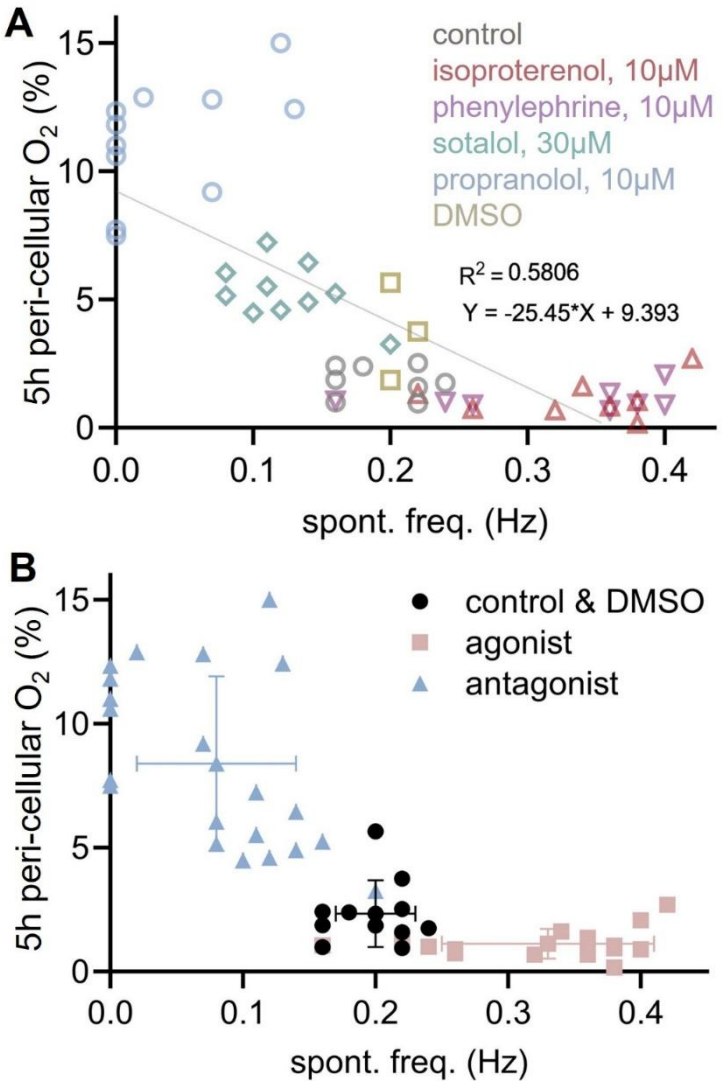


**Figure 5**. **Correlation of peri-cellular oxygen measurements and cardiac cellular activity. A.** Correlation plot of peri-cellular oxygen readings at 5 h of adrenergic treatment and cell spontaneous frequency (n=3-11 per group, samples colored by treatment). **B.** Grouped correlation plot for adrenergic antagonists, control and adrenergic agonists (n=11-21 per group); bars represent the standard deviations in either parameter per group.

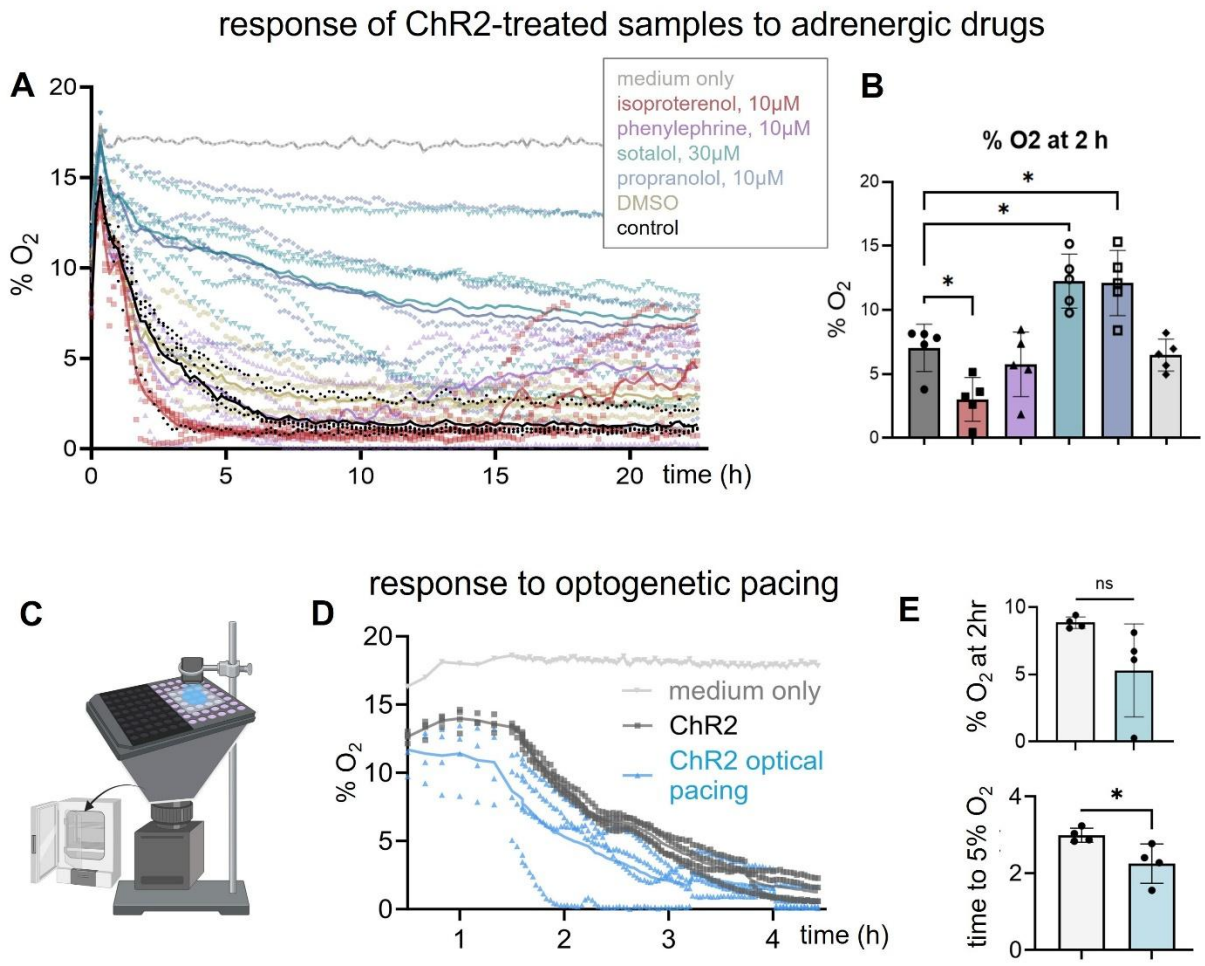


**Figure 6**. **Active perturbation of rate through optogenetic pacing and changes in pericellular oxygen. A.** Pericellular oxygen of adrenergic treated samples after ChR2 infection (n=5 per group except medium-only group). **B.** Summary of steady-state pericellular oxygen values at 2 h after treatment for all groups. One-way ANOVA with Dunnett's multiple comparisons showed significant differences between control and isoproterenol ($p = 0.0198$), sotalol ($p = 0.0022$), and propranolol ($p = 0.0029$). **C.** Diagram illustrating the setup for optical pacing within an incubator with peri-cellular oxygen measurement. **D.** Oxygen consumption comparison between optically paced and non-paced samples hiPSC-CMs (n=4 per group). **E.** Comparison of oxygen consumption metrics between optically paced and non-paced samples (top: peri-cellular oxygen level after about 2 h of optical pacing; bottom: time to reach 5% $O_2$ level); Unpaired t test was applied for statistical analysis, $p = 0.0338$.